Contents of this file

Figures S1 – S13

Introduction

In this supplementary, we find:

1. **the results for the three case studies that are not shown in the main text (Figure S1-S8):**

Cases 3: Malmbanan/E10 (Northern Sweden)

The first study area (5.5 × 5 km) is located southeast of Lake Torneträsk and northwest of Kiruna City (Figure 1). It covers a 5 km segment where the Malmbanan railway and the E10 highway run in close parallel. This area was deliberately kept small to reduce processing time while capturing diverse topography, boreal forest conditions, and the strong seasonal temperature gradients characteristic of northern Sweden. Along Malmbanan railway, both datasets indicate very slow uplift (below ~2 mm/year), although neither method yields coherent measurement points on the adjacent E10 highway, and EGMS-PS coverage is limited to short segments of the railway, reflecting sparse persistent scatterer availability.

Cases 4: E45 and regional railway (Southwest Sweden)

The fourth area, with a spatial extent like Case 3, is located southwest of Lake Vänern (Figure 1). This area includes a 5 km section of the E45 highway and a regional railway line. The land cover consists of a mixture of agricultural land, forest, and urban zones. This location lies within regions historically prone to landslides and rapid ground motion (Figure 1) (SHK, 2025b), providing conditions suitable for testing the sensitivity of InSAR measurements to climate-induced and geotechnical instability. In this case, Lödöse (Fig. S1), which is close to Case 1 (in the main text), both methods detect LOS displacement rates exceeding 5 mm/year on the E45 and the crossing regional railway, and given the proximity of these two cases, this indicates a broader zone of active ground motion affecting multiple corridors in the region. We also see ~4 mm/year subsidence on the Lödöse regional railway (Fig. S2).

Case 5: Stockholm Bypass (Förbifart Stockholm)

The fifth area corresponds to the E4 Stockholm Bypass, a major infrastructure project comprising ~17 km of underground motorway and 4 km of above-ground sections (See the project webpage here: https://www.trafikverket.se/vara-projekt/projekt-i-stockholms-lan/e4-forbifart-stockholm/). Similar to the Gothenburg case, this corridor represents a complex urban environment with ongoing or recent construction, providing a challenging test setting for evaluating InSAR-based ground-motion measurements in the vicinity of underground infrastructure. Along the Stockholm Bypass, neither method reveals pronounced surface motion, although dense vegetation leaves large portions of the corridor sparsely sampled. We also see a ~2.5 mm/year subsidence–uplift pattern around the 180th chainage of the Stockholm Bypass, more pronounced in the PS+DS results (Fig. S2).

For both Gothenburg and Stockholm, the analysis was performed within 100 m-wide corridors centered on the underground alignments.

2. **Also we show the relationship between RMSE/DEM and the distance to the centerline for all the cases (S9-S10).**
3. **Addistionally, we present the sensitivity of different InSAR solutions to the temporal coherence for the case of Lödöse (S11-S13).**

To better understand the impact of processing choices on the comparison between EGMS and locally processed InSAR measurements, we excluded DSs from our processing chain (we call it PS) conducted a sensitivity analysis for the Lödöse corridor (Figures S1–S3), focusing on (i) processing choice (EGMS (PS subset in Sweden), PS+DS, & PS) and (ii) temporal coherence thresholds (0.7, 0.5, and 0.3). These analyses are not intended to establish strict equivalence between processing chains, but rather to evaluate how methodological differences influence practical outcomes such as spatial coverage, accuracy, and ground motion patterns.

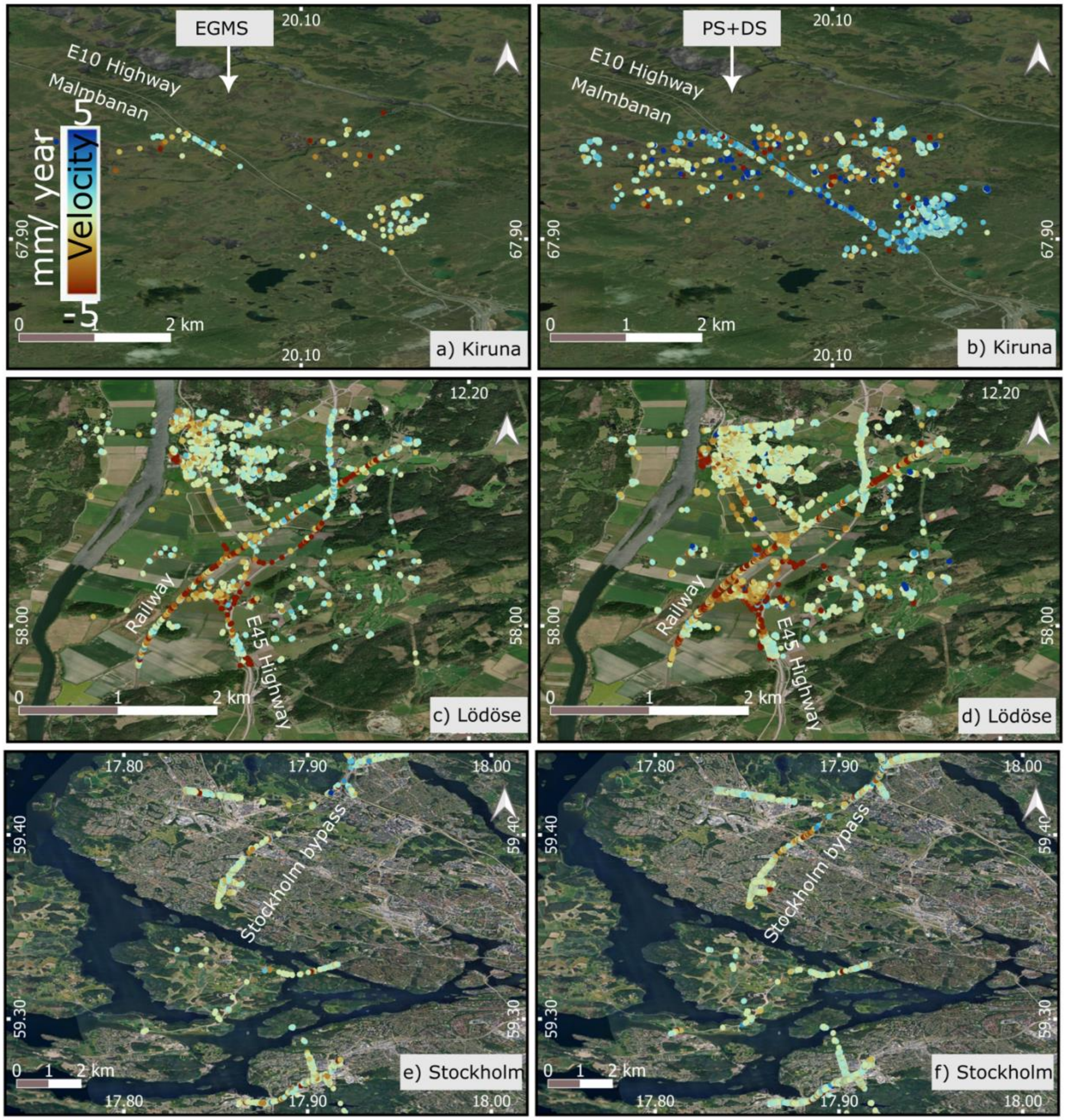

Figure S1. *The ground motion velocity maps between 2020 and 2024 from the EGMS-PS Calibrated LOS product on the left column, and from the PS+DS approach on the right column, illustrating the local displacement patterns around the rail and road segments analyzed in this study:* ***(a-b)*** *a section of Malmbanan railway & E10 highway, north-west of Kiruna City,* ***(c-d)*** *E-45 highway and regional railway, east of Lödöse City,* ***(e-f)*** *Stockholm underground Bypass (Förbifart Stockholm) along E4 highway. The basemap for panels a-d was designed and developed by Esri, Sources: Esri, Maxar, GeoEye, Earthstar Geographics, CNES/Airbus DS, USDA, USGS, AeroGRID, IGN, and the*

GIS User Community | Powered by Esri. The basemap for panels e-f: Imagery © 2026 NASA, Map data © 2026 Google.

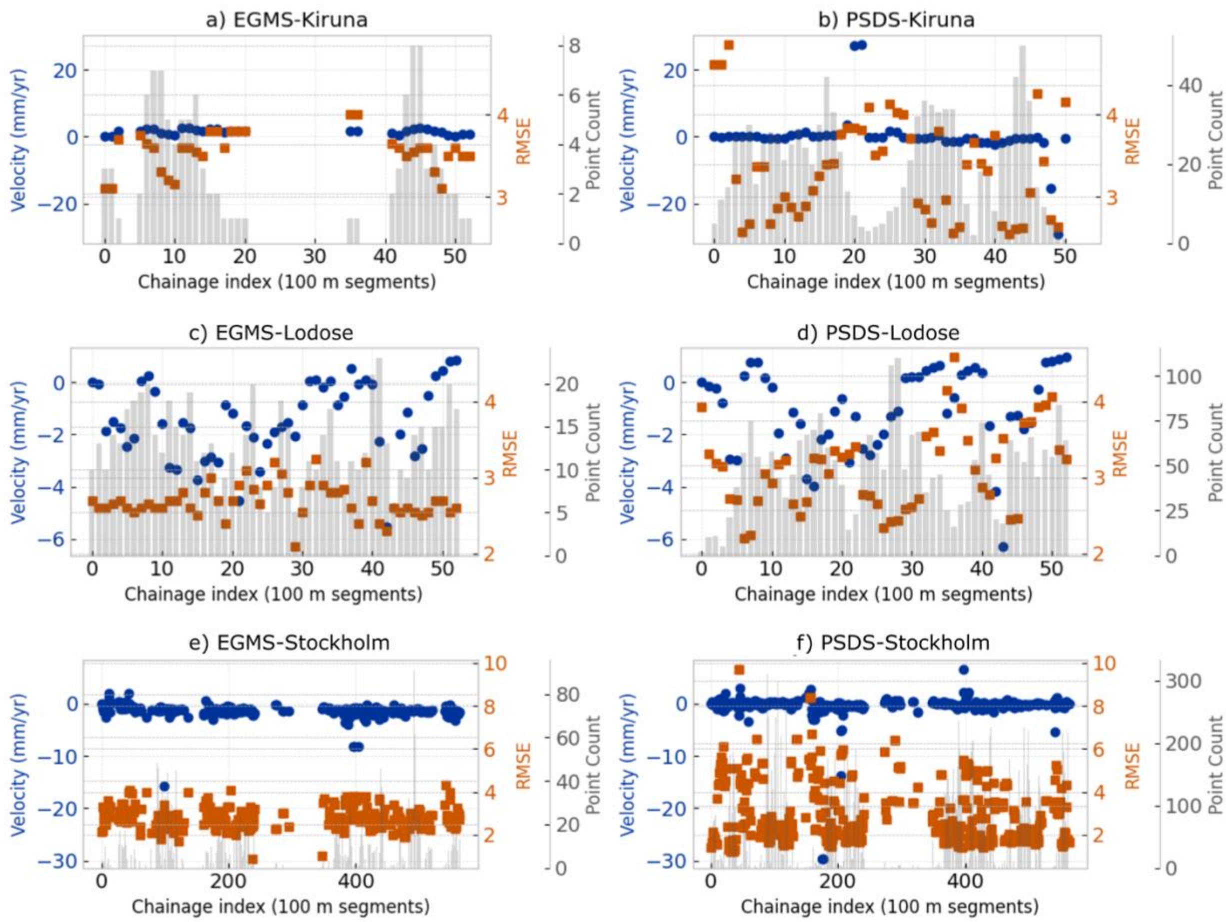

Figure S2. *Summary statistics (median) of velocity and displacement RMSE every 100 m chainage along the corridors, with EGMS (PS subset in Sweden) (**left panels**) and PS+DS (**right panels**). Left axes show LOS velocity referenced to the first chainage; right axes show RMSE (mm), with grey bars indicating point counts. Both EGMS (PS subset in Sweden) and PS+DS method capture similar displacement patterns across the corridors, including localized subsidence in Lödöse (regional railway) (~4 mm/year) and the Stockholm Bypass (~2.5 mm/year).*

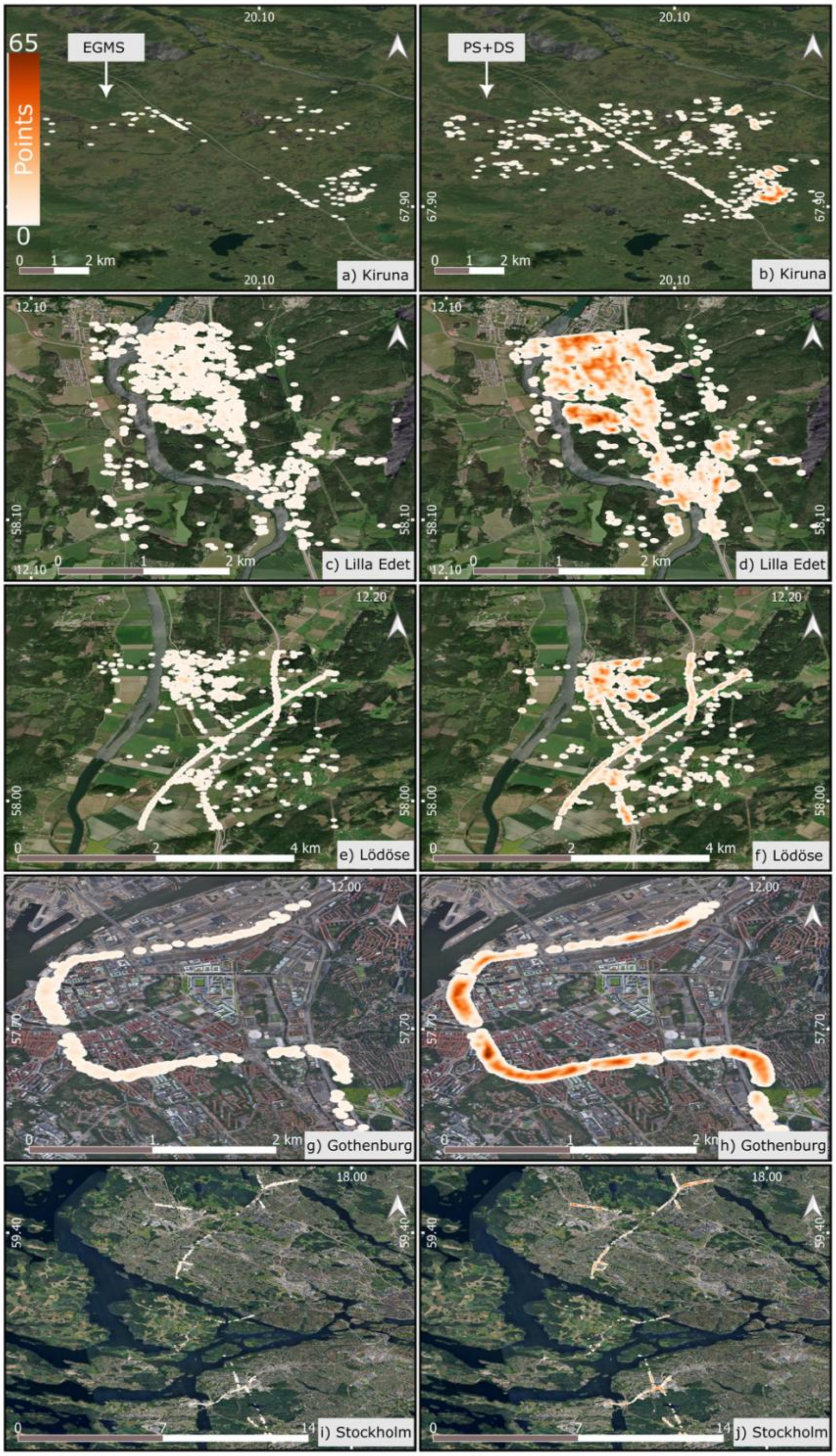

Figure S3. *Point-count heatmaps (number of points in a 50-m radius) for the five case studies with EGMS (PS subset in Sweden),* ***left column****, and PS+DS phase-linking,* ***right column****. The basemap for panels a-f was designed and developed by Esri, Sources: Esri, Maxar, GeoEye, Earthstar Geographics, CNES/Airbus DS, USDA, USGS,* *AeroGRID, IGN, and the GIS User Community | Powered by Esri. The basemap for panels g-j: Imagery © 2026 NASA, Map data © 2026 Google.*

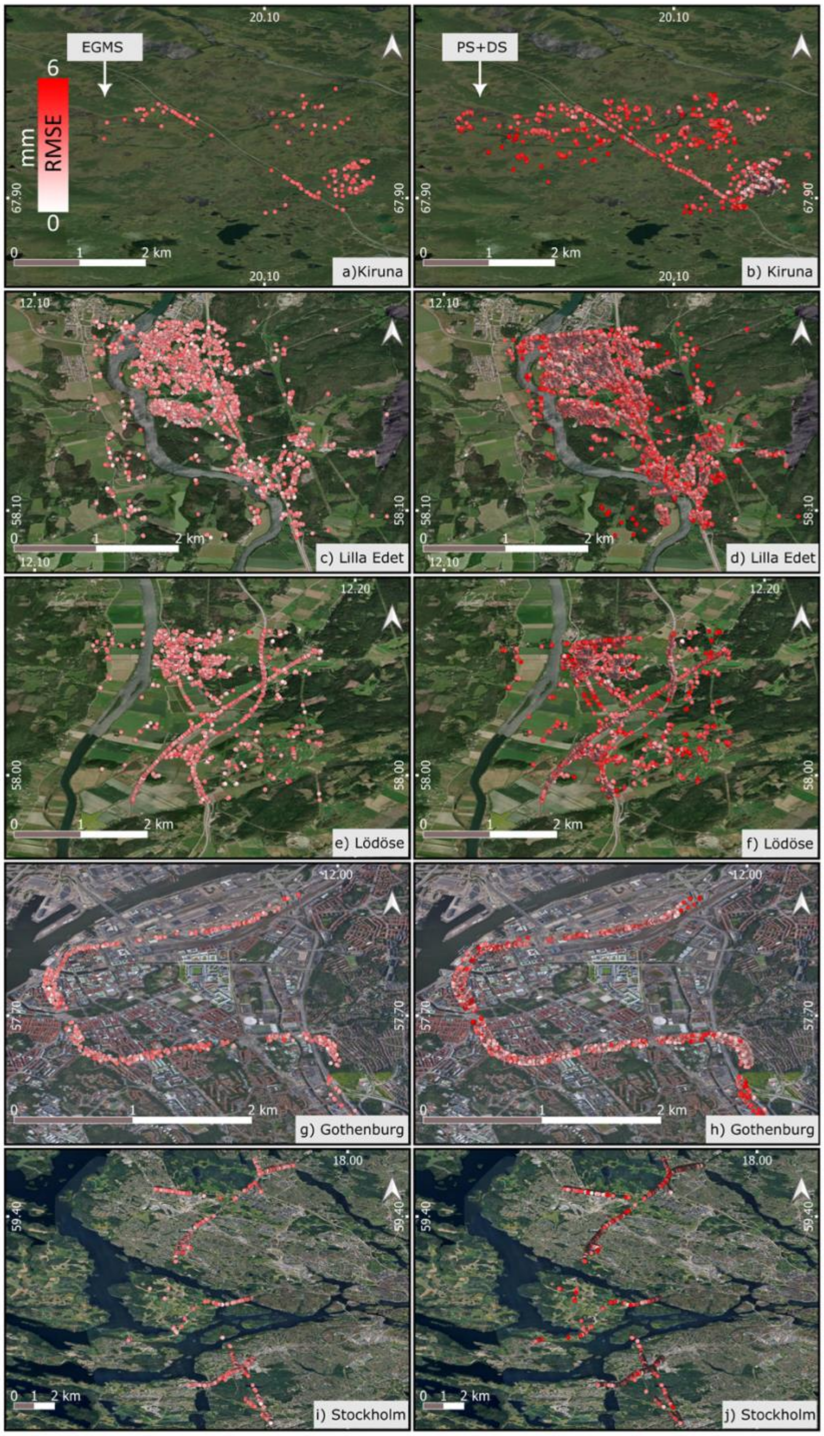

Figure S4. *RMSEs of the displacement time series for EGMS (PS subset in Sweden)* ***(left column)*** *and PS+DS (****right column****). Both the EGMS (PS subset in Sweden) and PS+DS exhibit similar RMSE levels (generally ≤ 6 mm in the LOS direction), with lower values for EGMS (PS subset in Sweden) due to the PS-only selection in Sweden. The basemap for panels a-f was designed and developed by Esri, Sources: Esri, Maxar, GeoEye, Earthstar Geographics, CNES/Airbus DS, USDA, USGS, AeroGRID, IGN, and the GIS User Community | Powered by Esri. The basemap for panels g-j: Imagery © 2026 NASA, Map data © 2026 Google.*

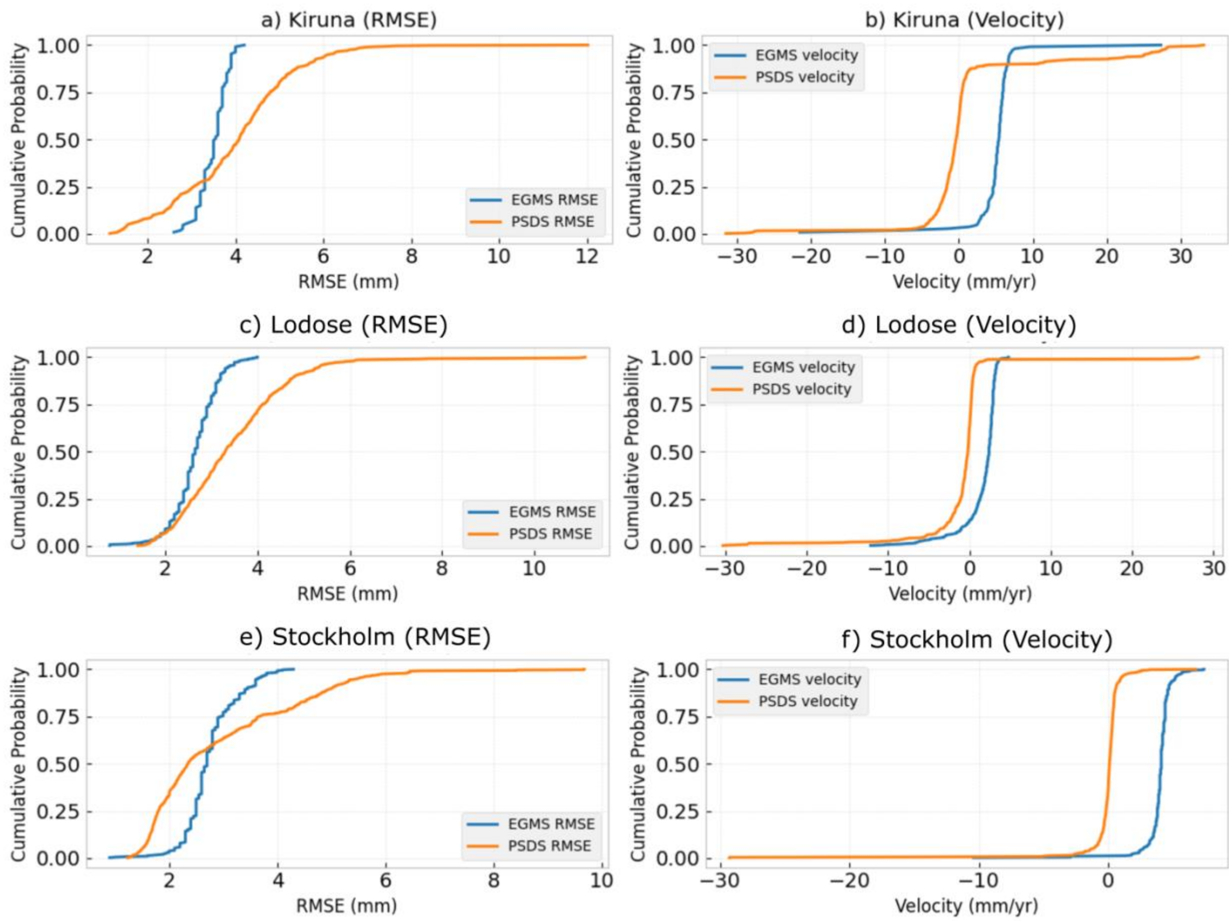

Figure S5. *Cumulative probability distributions of RMSE (****left panels****) and velocity (****right panels****) for the EGMS (PS subset in Sweden) and PS+DS. Both values are medians within 100 × 100 m grid cells. Velocity distributions show similarly steep curves for both datasets, indicating comparable displacement behavior along the corridors.*

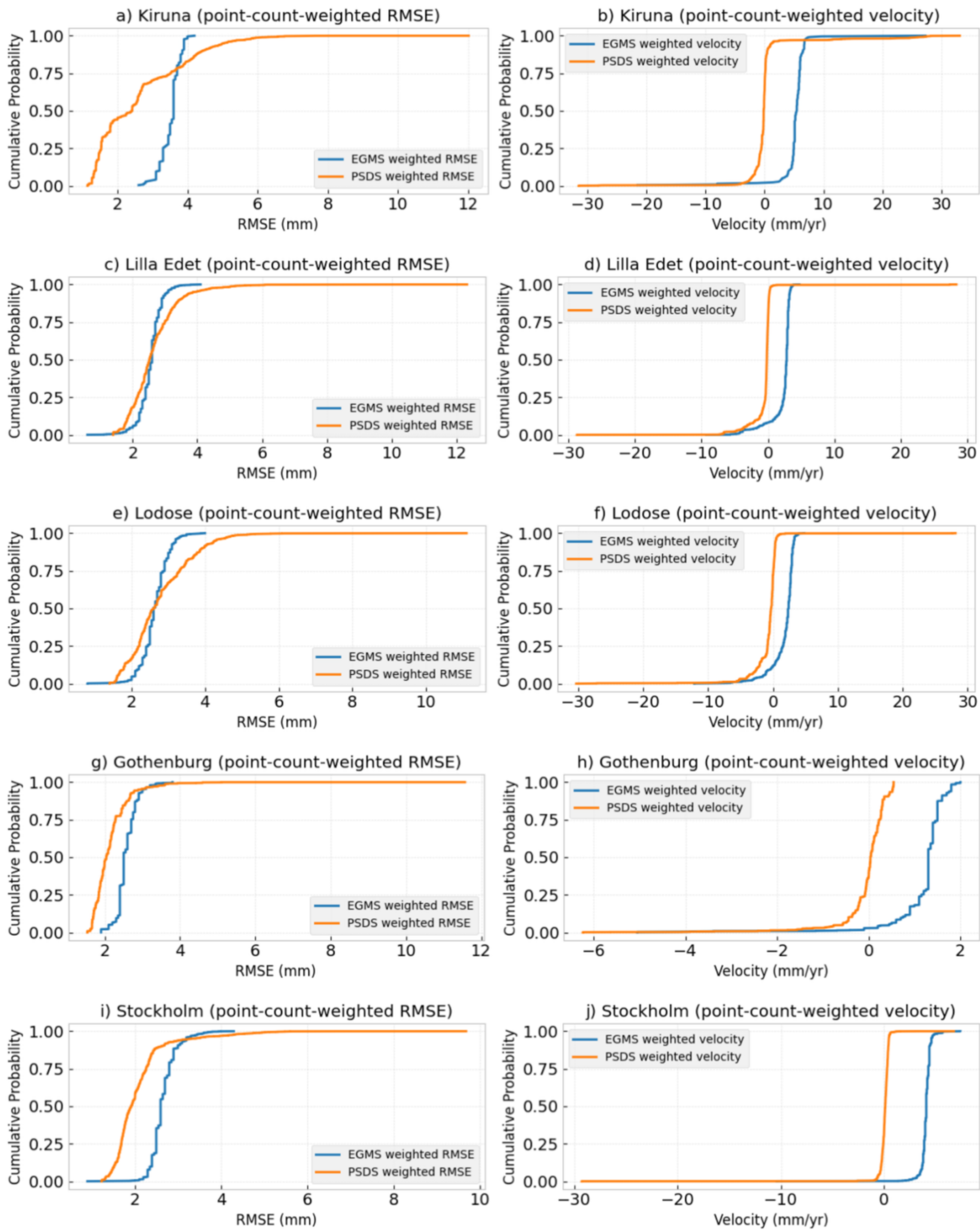

Figure S6. *Point-count–weighted cumulative probability distributions of RMSE (**left panels**) and velocity (**right panels**) for the EGMS-PS and PS+DS. All values are medians within 100 × 100 grid cells.*

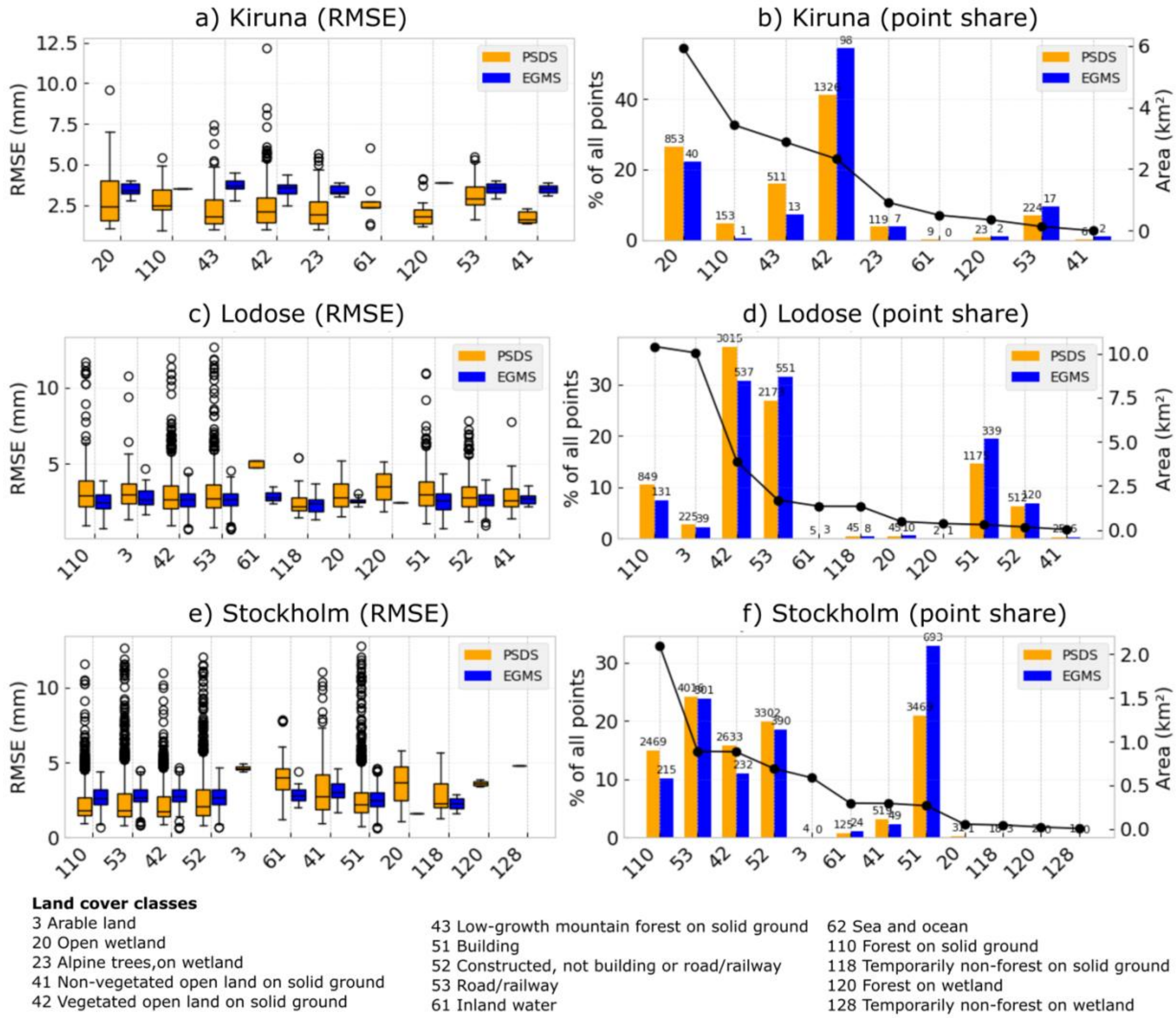

Figure S7. Left panels: *RMSE boxplots for EGMS-PS and PS+DS across land-cover classes.* ***Right panels:*** *point-percentage (left axis) and land-cover area (right axis). The numbers on top of bars are the number of measurement points. Points appearing over water bodies originate from bridges, near-shore pixels, or sidelobes of onshore scatterers.*

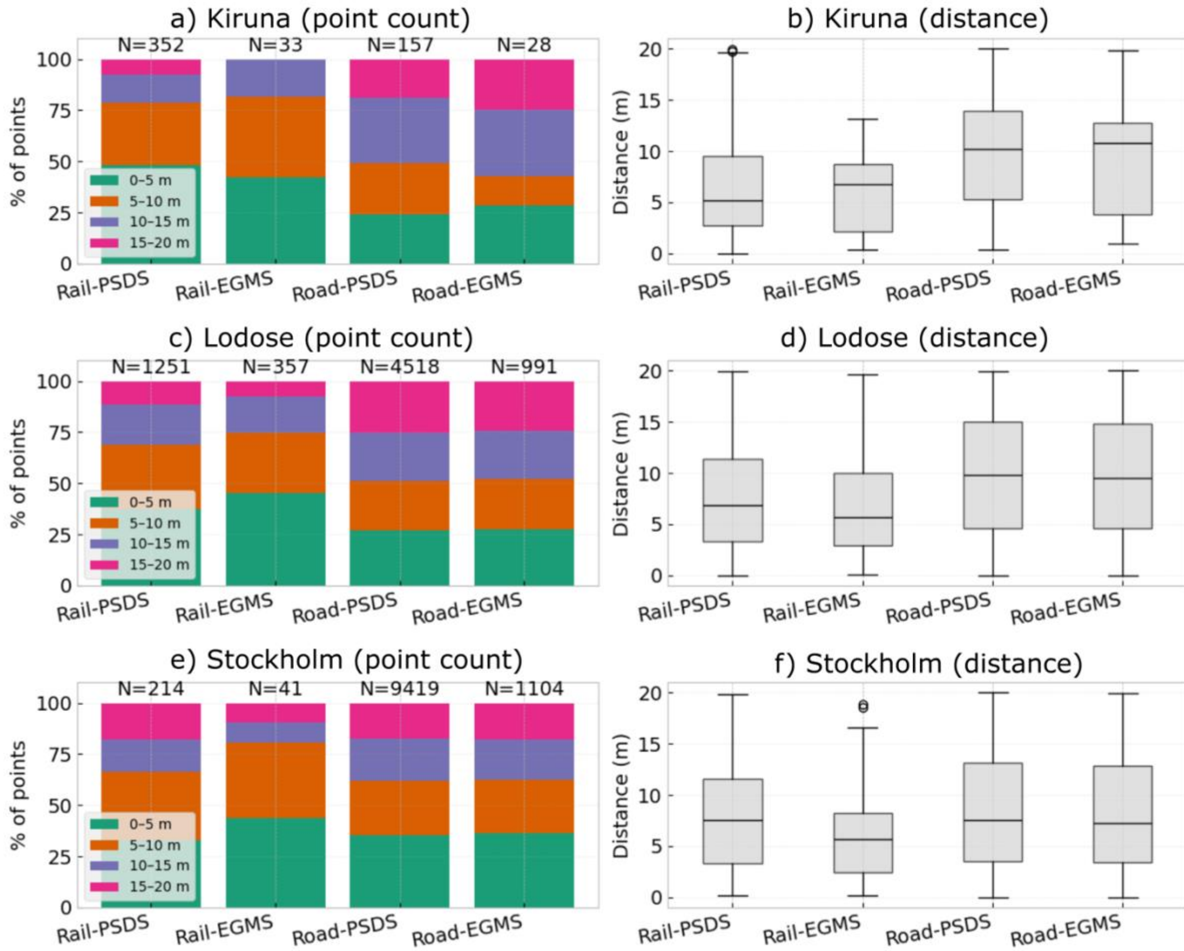

Figure S8. Left panels: *stacked bar charts showing the percentage of points within 0–5, 5–10, 10–15, and 15–20 m of road and railway centerline, based on data clipped to a 20 m corridor around all transport segments. The numbers on top of bars are the number of measurement points.* ***Right panels:*** *boxplots of distance to centerline.*

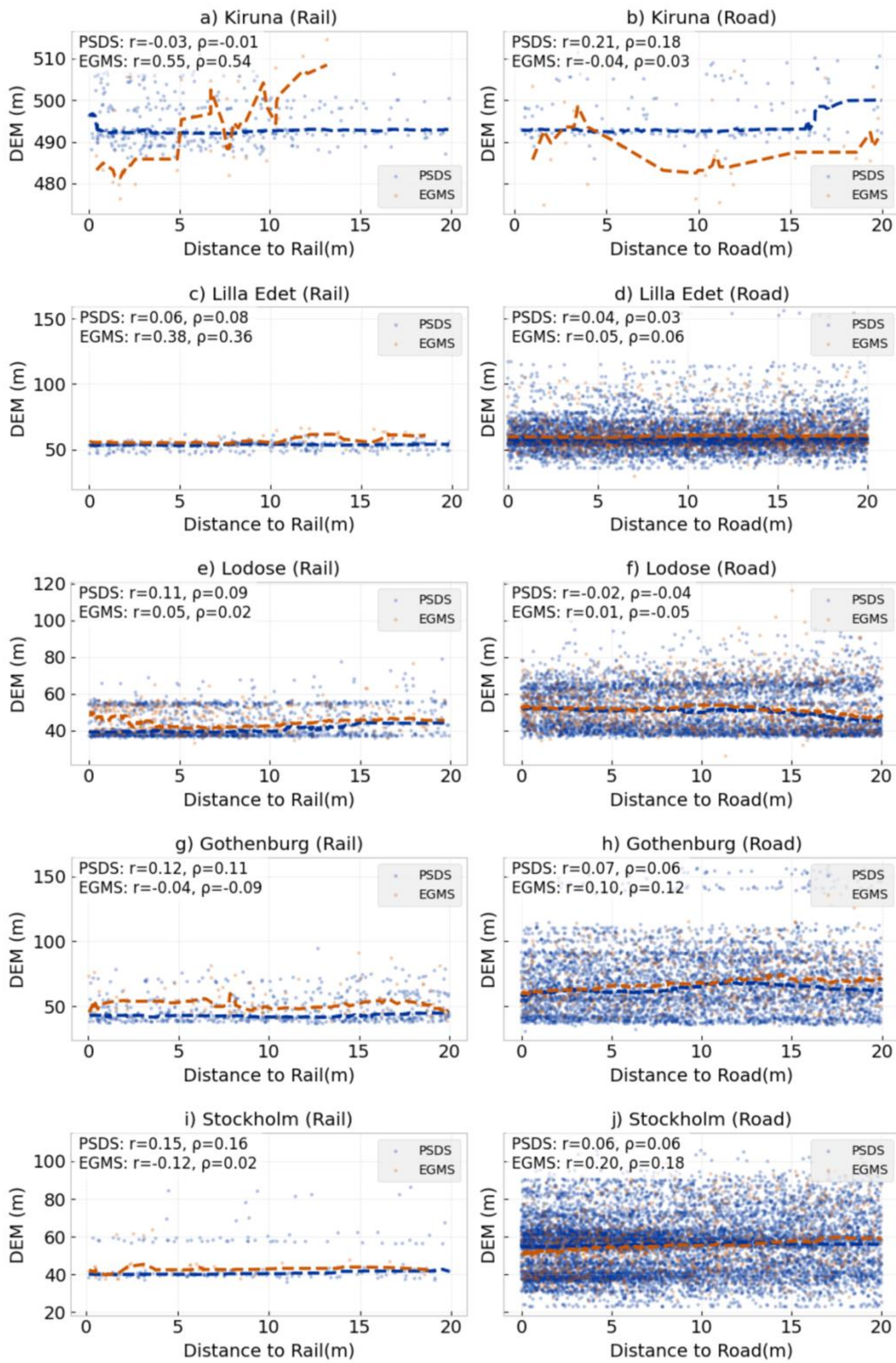

Figure S9. *Scatter plots of RMSE versus distance to railway (**left column**) and distance to road (**right column**) centerline (20 m corridor). r and ρ are Pearson and Spearman correlations respectively.*

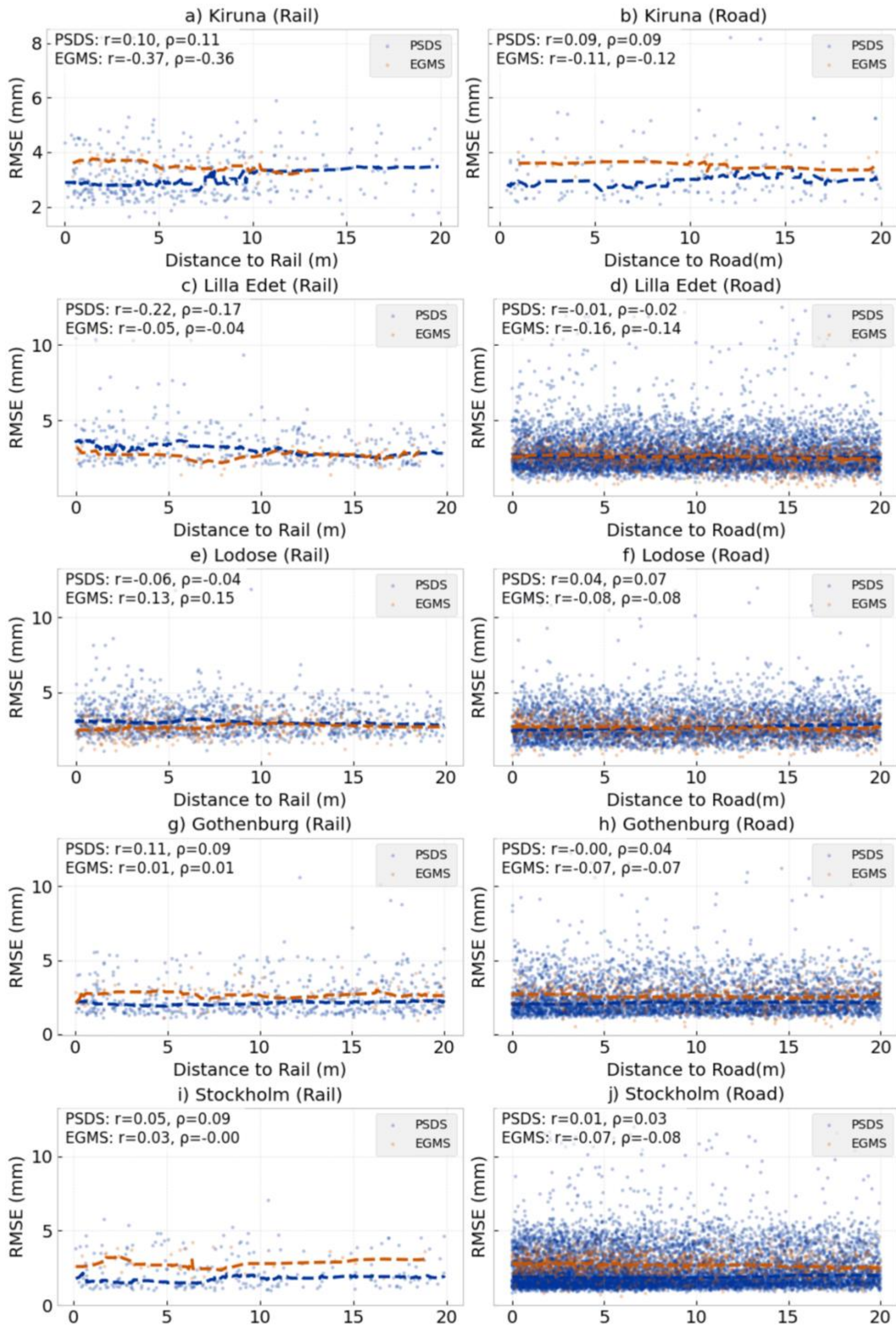

Figure S10. *Scatter plots of elevation (DEM) versus distance to railway (**left column**) and distance to road (**right column**) centerline (20 m corridor). r and ρ are Pearson and Spearman correlations respectively.*

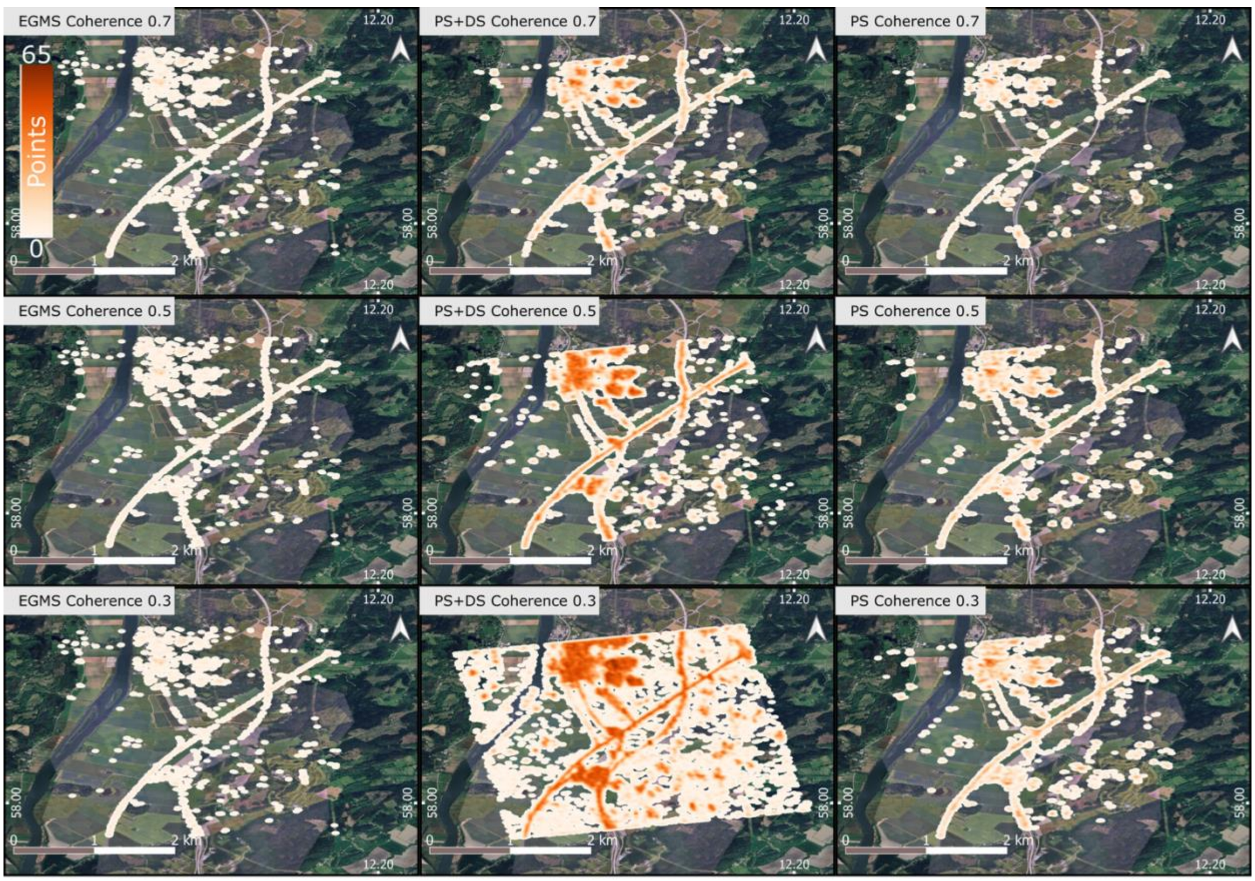

Figure S11. Point-count heatmaps (number of points in a 50-m radius) for the case of Lödöse comparing EGMS (PS subset in Sweden) (left column), PS+DS phase-linking (middle column), and locally processed PS (right column), with different temporal coherence thresholds: 0.70 (first row), 0.5 (second row), and 0.3 (last row). The basemap: Imagery © 2026 NASA, Map data © 2026 Google.

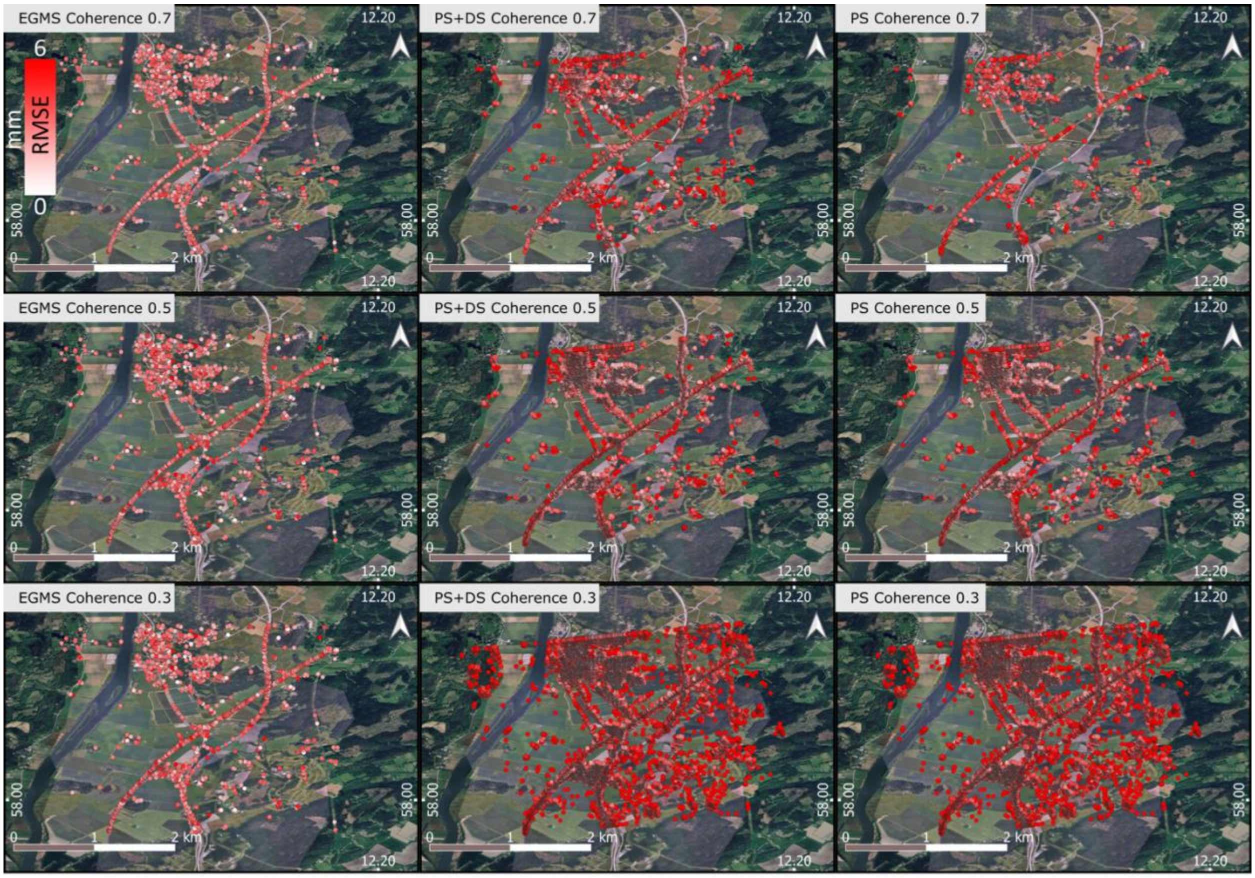

Figure S12. RMSEs of the displacement time series for the case of Lödöse comparing EGMS (PS subset in Sweden) (left column), PS+DS phase-linking (middle column), and locally processed PS (right column), with different temporal coherence thresholds: 0.70 (first row), 0.5 (second row), and 0.3 (last row). The basemap: Imagery © 2026 NASA, Map data © 2026 Google.

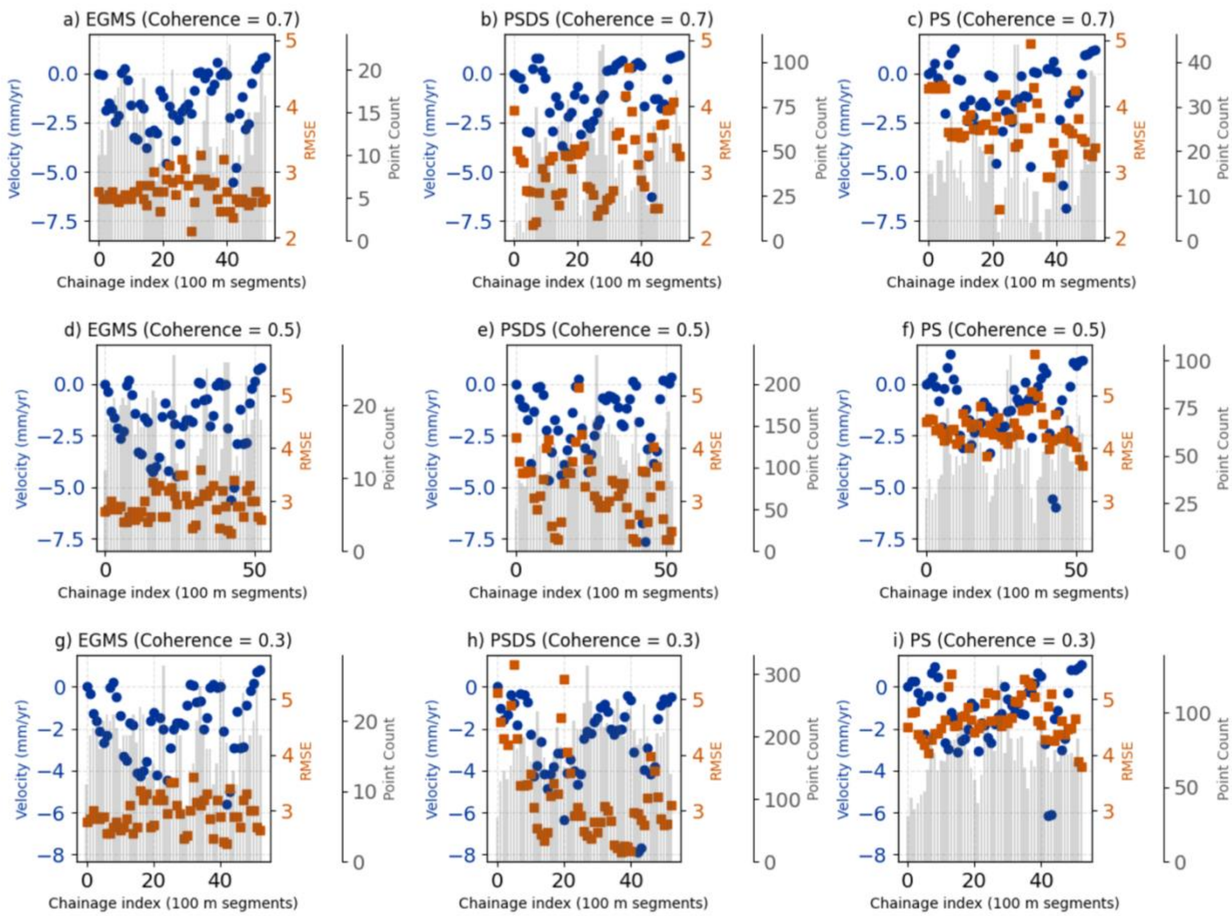

Figure S13. Summary statistics (median) of velocity and displacement RMSE every 100 m chainage along the corridors, for the case of Lödöse comparing EGMS (PS subset in Sweden) (left column), PS+DS phase-linking (middle column), and locally processed PS (right column), with different temporal coherence thresholds: 0.70 (first row), 0.5 (second row), and 0.3 (last row). Left axes show LOS velocity referenced to the first chainage; right axes show RMSE (mm), with grey bars indicating point counts.